Human Molecular Genetics, 2001, Vol. 10, No. 10 **1039–1048**

Transgenic mice with an expanded CAG repeat controlled by the human AR promoter show polyglutamine nuclear inclusions and neuronal dysfunction without neuronal cell death

Hiroaki Adachi[1], Akito Kume[1], Mei Li[1], Yuji Nakagomi[2], Hisayoshi Niwa[1], Jun Do[1], Chen Sang[1], Yasushi Kobayashi[1], Manabu Doyu[1] and Gen Sobue[1,+]

[1]Department of Neurology, Nagoya University School of Medicine, 65 Tsurumai-cho Showa-ku, Nagoya 466-8550, Japan and [2]Laboratory of Electron Microscopy, Aichi Medical University, Aichi 480-1195, Japan

Received 18 December 2000; Revised and Accepted 7 March 2001

We generated transgenic mice that expressed a highly expanded 239 polyglutamine (polyQ) repeat under the control of the human androgen receptor promoter. These transgenic mice developed progressive neurological phenotypes of muscular weakness and ataxia, small body size and short life-span. PolyQ nuclear inclusions (NIs) were remarkable and widespread but found in selective regions of the central nervous system (CNS) such as the spinal cord, cerebrum and cerebellum as well as in selective peripheral visceral organs. This distribution pattern resembled that of spinal and bulbar muscular atrophy somewhat, but was more widespread. In neuronal tissues, NIs were present in astrocytes as well as neurons. Cytoplasmic and axonal inclusions were not observed. In the CNS regions with abundant NIs, neuronal populations were well-preserved, and neither neuronal cell death, reactive astrogliosis nor microglial invasions were detected. These findings suggest that polyQ alone can induce the neuronal dysfunction that precedes gross neuronal degeneration and provides a clue for investigating molecular mechanisms that underly the pathway to neuronal dysfunction from polyQ expansion.

INTRODUCTION

Spinal and bulbar muscular atrophy (SBMA) is a late-onset X-linked motor neuron disease caused by an expansion of polyglutamine (polyQ) repeat in androgen receptor (AR) (1), one of the neurodegenerative diseases caused by a polyQ expansion, such as Huntington's disease (HD), SCA1, 2, 3, 6, 7 and dentatorubural-pallidoluysian atrophy (2,3). The major neuropathological finding of SBMA is loss of bulbar and spinal motor neurons showing progressive limb muscular atrophy and difficulty in swallowing and speech. Mild sensory impairment due to neuron degeneration (4,5), testicular atrophy, gynecomastia and feminized skin change are also present (4,5). An inverse correlation between age of onset and expansion of a CAG repeat has been reported (6–8). Nuclear inclusions (NIs) consisting of mutant and truncated AR with expanded polyQ in combination with many components of ubiquitine-proteasome and molecular chaperone pathways are found in the residual motor neurons in the brain stem and spinal cord as well as in skin, testis, kidney, heart and some other visceral organs of SBMA patients (9,10).

A neuronal cell line expressing truncated AR with expanded-polyQ was found to present nuclear aggregates of mutant AR and apoptosis by TUNEL staining (11). However, only extremely truncated AR with highly expanded polyQ induced NIs and apoptosis, suggesting that the expanded polyQ plays an essential role in aggregate formation and apoptosis. Both NIs and apoptosis were well prevented by co-expression of molecular chaperons Hsp70, Hsp40 and others with truncated AR harboring a highly expanded polyQ (11,12), also suggesting that the expanded polyQ plays a central role in cell toxicity. In many other *in vitro* models of CAG repeat diseases, NIs and apoptosis have also been demonstrated, but aggregate formation and apoptosis are not necessarily linked (13,14). However, a functional impairment without apoptosis can be present in these *in vitro* models (15).

An *in vivo* transgenic mouse model with a transgene harboring an expanded CAG repeat for HD, SCA1, SCA3 and SCA7 driven by potent promoters (16–23) showed evidence of neuronal degeneration and neuron loss accompanied by apparent astrogliosis (17–21,23). However, other transgenic mouse models of CAG repeat diseases showed neuronal dysfunction without acute neurodegeneration resulting in neuron loss and astrogliosis (16,22,24,25). Furthermore, even in the transgenic models with neuron loss, a marked functional impairment of neurons such as altered expression of transcriptional factors preceding the neuron loss has been documented (26). In addition, non-apoptotic neurodegeneration has been recently reported to induce neuronal dysfunction similar to the HD phenotype in a transgenic mouse model of HD (17). These findings suggest that the causative gene products with an

[+]To whom correspondence should be addressed. Tel: +81 52 744 2385; Fax: +81 52 744 2384; Email: sobueg@tsuru.med.nagoya-u.ac.jp

expanded polyQ repeat can induce functional impairment of neurons without neuronal cell death. The expanded polyQ may play a central role in such functional impairment. The molecular mechanism for the eventual neuronal cell death in CAG repeat diseases has not been well understood, particularly in relation to apoptosis, but the neuronal dysfunction which may precede neuronal cell death is important from the therapeutic point of view. The role of the expanded polyQ in these functional impairments without neuronal cell death, particularly in the *in vivo* model, remains to be identified. This process can be investigated using a transgenic mouse with a highly expanded CAG repeat controlled by the promoter for the causative gene of the disease.

In this study, we generated the transgenic mouse model with an extremely expanded 239 CAG repeat alone under the control of a human AR promoter. Two lines of these transgenic mice expressed strong phenotypes of neuronal dysfunction and widespread polyQ NIs including in motor neurons, but showed neither neuronal cell death nor any evidence of apoptosis.

RESULTS

Fragment used for transgene

The 5′-flanking region of the human AR gene (GenBank accession no. G508476 of the promoter region and GenBank accession no. G178627 of the human AR mRNA) was used as the promoter to direct the expression of the transgene. The human growth hormone polyadenylation signal was included in this construct to allow for proper processing of the transgene mRNA (Fig. 1A). The microinjection fragment was 4.7 kb and had the 3.4 kb 5′-flanking region of the human AR gene, 239 CAG repeat, FLAG epitope sequence and human growth hormone polyadenylation signal sequence.

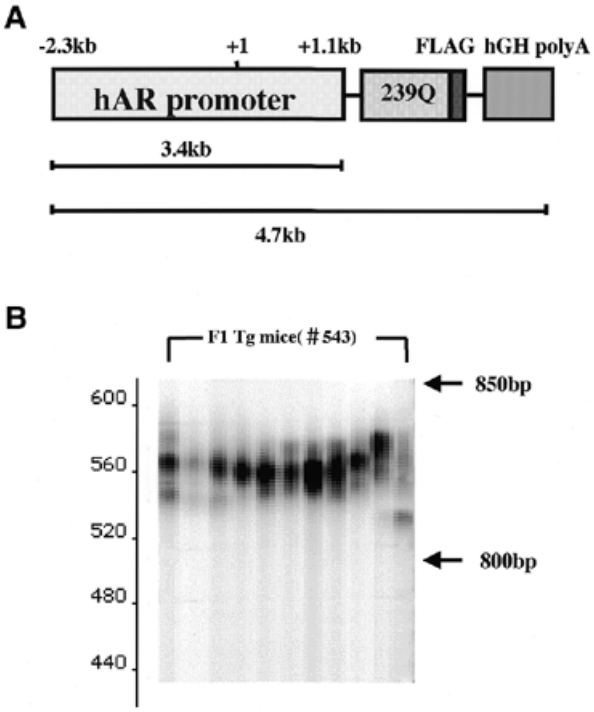

Figure 1. Schematic view of transgene constructs and measurement of the size of the CAG expansion in transgenic mice. (**A**) Schematic view of transgene constructs. The 4.7 kb microinjected fragment was composed of a 3.4 kb human genomic fragment containing AR promoter sequences, a 239 CAG repeat, the FLAG epitope sequence and human growth hormone polyadenylation signal sequence. (**B**) Measurement of the size of the CAG expansion in transgenic mice. Each lane contains amplified product using a Texas Red-labeled primer from each F_1 mouse DNA (AR-239Q-#543). The primary PCR product obtained from each animal showed a slight variation in CAG repeat length, indicating minor meiotic instability of CAG repeat size in the transgene.

AR 239Q mice exhibit a progressive neuronal phenotype

We generated four lines of transgenic mice that expressed 239Q under the control of the human AR promoter. Two transgenic lines (AR-239Q-#538 and AR-239Q-#543), which contained one and 50 copies of the transgene, respectively, developed a neurological phenotype, but the other two lines did not show any neurological symptoms. The 239 CAG repeat in the transgene was assessed by the PCR amplification on the tail DNA using a fluorescently labeled primer, and subsequent size determination using a Hitachi sequencer showed slight intergenerational change of repeat size, indicating a minor meiotic instability of the CAG repeat size in the transgene (Fig. 1B). Two lines, #543 and #538, exhibited small body size, short life-span (Fig. 2) and motor weakness with dragging of the hind legs, decreased walking speed, truncal and limb incoordination and reduced cage activity (Fig. 3). These phenotypes were apparently developed within 4–8 weeks of birth in both lines, and gradually became profound at 8–16 weeks, while the severity of each phenotypic expression was somewhat variable among the mice. Progressive impairment of the rotarod task, which appeared within 8 weeks of birth, and the subsequent decline was monophasic (Fig. 3A). In the advanced stage, the mice could not stand on their hind limbs, fell when walking, and reached around to groom their back resulting in a somersault. Their body weight was also 60–70% below that of their littermates (Fig. 2A). Age at death was between 10 and 16 weeks (Fig. 2B), with the cause of death generally unknown.

Expression of transgene

Expression of the transgene was assessed by RT–PCR and western blotting analysis using the primer sets for the FLAG gene and a polyclonal antibody to FLAG. Two lines, #543 and #538, with neuronal phenotypes, expressed the transgene to a variable extent in cerebrum, cerebellum, spinal cord, pituitary, lung, eye and skin (Fig. 4 and Table 1), but not in the testis, pancreas, heart, liver, muscle, kidney, intestine or spleen (Fig 4 and Table 1). Although the distribution pattern of the transgene product varied somewhat with the transgenic line, the results indicated that expression of the transgene was not universal, but was restricted to the subset of the tissues. The FLAG product was only detected in the pellet fraction spun at 2500 *g*, and only appeared at the top of the western blotting gel (Fig. 4B), indicating that most of the transgene products were present as aggregates retained at the top of the stacking gel (Fig. 4B). Blocking of anti-FLAG antibody with the FLAG peptide reduced the density in all of the tissues that expressed the transgene products (data not shown).

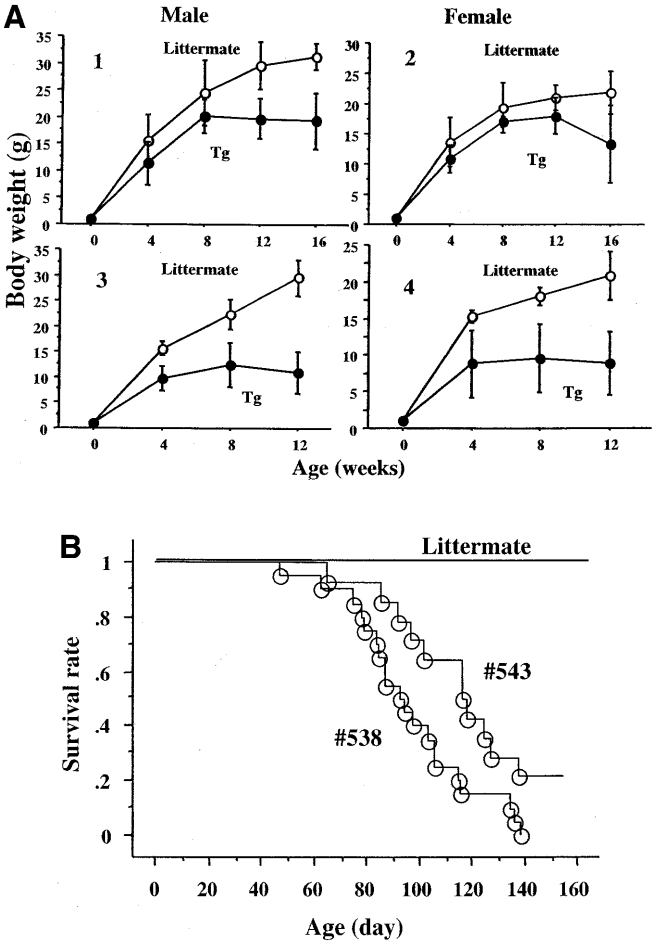

Figure 2. Body weight and survival rate of transgenic mice. (**A**) Body weight change in terms of aging. At birth, the transgenic mice are indistinguishable from their littermates in body weight, but gradually lose weight with advancing age. 1 and 2, AR-239Q-#543; 3 and 4, AR-239Q-#538. Results are expressed as mean ± SD. (**B**) Survival rate of transgenic mice. 50% mortality for #543 and #538 was at 118 and 100 days, respectively.

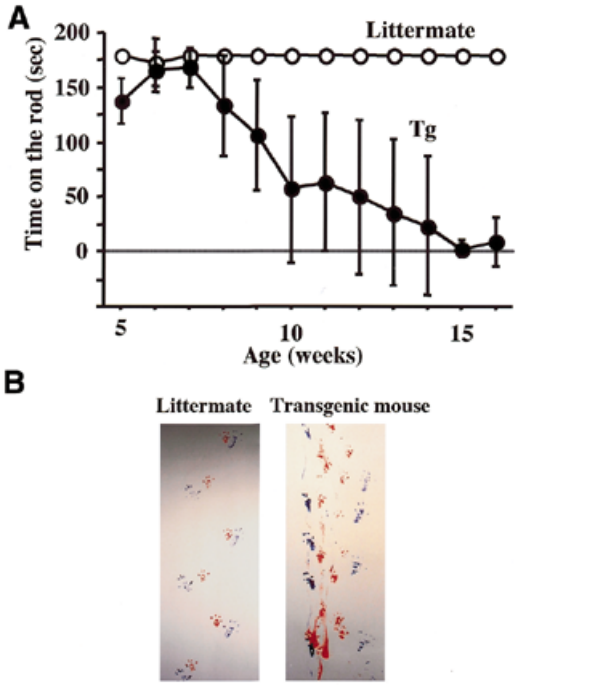

Figure 3. Neurological dysfunction in transgenic mice. (**A**) Lowered performance on the rotarod apparatus in transgenic mice. Transgenic mice (black; $n = 6$, AR-239Q-#543) and littermates (white; $n = 6$) were tested weekly up to 16 weeks by measuring the time spent on the rod. Results are expressed as mean ± SD. (**B**) Footprint of 12-week-old AR-239Q-#543 male mouse. The transgenic animal exhibits motor weakness and incoordination with dragging of the hind legs and wide-based ataxic gait.

PolyQ NIs and neuropathology

The brain weight at 12 weeks in the transgenic mice was consistently smaller than that of their littermates [421 ± 10.8 mg ($n = 3$) versus 499 ± 2.5 mg ($n = 3$)]. The spinal cord and cerebellum were also smaller than those in their littermates. Although the amount of central nervous system (CNS) tissue was generally small, there was no evidence of active neuronal degeneration nor of reactive astrogliosis. We quantified the Nissle stain-positive neuronal population and the immunoreactive NIs in the lumbar spinal ventral horn, frontal cortex and cerebellar granular cell layers of the cerebellum from 12-week-old transgenic mice and their littermates. The neuronal cell population in these regions of the transgenic mice was well preserved or even elevated in the advanced stage (Fig. 5), while the NIs were abundant, as described below (Fig. 5). Immunohistochemistry with anti-GFAP antibody and microglial marker anti-CD68 antibody did not show any reactive astrogliosis or reactive microglial assembly in the CNS tissues of the transgenic mice. TUNEL staining did not show any positive nuclear staining in the transgenic mouse CNS tissues. These findings indicated that neuronal cell death (particularly neuronal cell apoptosis and neuron loss) was not present in these transgenic mice. The peripheral visceral organs were also normal in appearance and TUNEL staining did not show any pathological nuclear staining.

The most striking observation was widespread occurrence of polyQ NIs. The NIs were distributed in the neuronal cell nuclei in the cerebrum, cerebellum, brain stem and spinal cord, but to a lesser extent or not at all in the basal ganglia of pallidum and striatum (Fig. 6A and Table 1). Some inclusions were seen in the ependymal cells. The NIs were most prominent in neurons of the fronto-parietal cortex and cerebellar granular cell layer, and in motor neurons in the spinal cord (Fig. 6A and Table 1). In other CNS tissues, NIs were less prominent or absent (Table 1). In these regions with marked occurrence of NIs, the NIs were also prominently observed in the nuclei of the glial cells, particularly of astrocytes stained with GFAP (Fig. 6A and Table 1). These neuronal and glial NIs were similar in size and structure; granular materials densely aggregate without a limiting membrane or filamentous materials on electron microscopic immunohistochemistry (Fig. 6B), and the electron microscopic structure of NIs was very similar to those observed in SBMA patients (10). These NIs were positive for ubiquitin (Fig. 6A) and colocalized with proteasome components (20s, PA28α, PA28γ; data not shown). No cytoplasmic or axonal inclusions were observed in the neuropil. Neurons and astrocytes which develop the NIs were normal in appearance

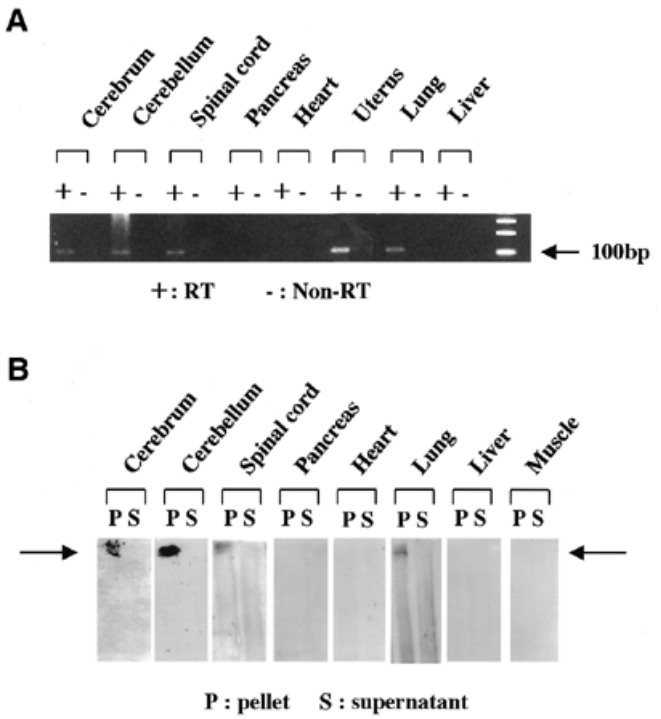

Figure 4. Transgene expression in the transgenic mice. (**A**) RT–PCR analysis of RNA from transgenic mice. Total RNA was prepared from each tissue of 12-week-old transgenic mice. The transgene was expressed in the cerebrum, cerebellum, spinal cord and lung to variable degrees among the tissues. (**B**) Western blot analysis of expression using the rabbit anti-octapeptide epitope tag. FLAG product was only detected in the pellet fraction of 2500 *g* and at the top of the stacking gel. The expression of FLAG products is detectable in the cerebrum, cerebellum, spinal cord and lung. Representative tissues were selected from #543 and #538.

and shape. In the developmental profile, NIs in CNS tissues were very few at birth, but gradually increased in frequency with advancing age to reach a plateau level at 8–10 weeks old (data not shown).

NIs were also observed in peripheral visceral organs such as the pituitary, lung, skin, adrenal gland and peritoneal tissue (Fig. 6A and Table 1). However, no NIs were detected in the kidney, testis, heart, gastrointestinal tissues, thymus or spleen (Table 1). These NI-distribution patterns also indicated that NIs are not ubiquitous in peripheral tissues but restricted to particular organs. All inclusions were restricted to the nuclei, and were not observed in the cytoplasm of the peripheral tissues. Immunohistochemical and ultrastructural characteristics of peripheral tissue NIs were similar to those in the CNS.

DISCUSSION

Transgenic mice with a progressive neurological phenotype and widespread polyQ NIs were generated by the introduction of an extremely expanded pure CAG repeat under the control of a human AR promoter. Widespread but tissue-restricted mRNA and protein expression was observed, and the mRNA and protein expression levels were variable in extent among the tissues. These expression levels were fairly well correlated with the distribution of polyQ NIs and of so far reported AR expression in mice (27), suggesting that similar transacting factors for human AR promoter worked in this mouse model. The polyQ NIs were not observed in either the neuropil or cytoplasm, but they were exclusively present in the nuclei, which agreed well with the findings in SBMA patients (9,10,28). The neuronal polyQ NIs occurred prominently in the frontal and parietal cortex, cerebellar granular cells and spinal motor neurons, which was more widespread than those of SBMA patients (9,10), but restricted to certain regions of the CNS. Despite widespread distribution of NIs in the peripheral visceral tissues, they were also restricted to subsets of organs, and somewhat resemble those observed in SBMA patients (10). Our transgenic model with pure and extremely expanded polyQ under the control of human AR promoter indicated that polyQ alone was sufficient to express widespread polyQ NIs and neuronal phenotype, while NIs were not ubiquitous but rather restricted to certain CNS regions and a certain subset of peripheral tissue organs. This observation suggests that human AR promoter activity also contributes to the selective tissue distribution of pathology. Recent observations on the transgenic mice with full-length DRPLA or HD genes suggested that the presence of tissue-specific proteolytic cleavage of these gene products contributes to the expression of the tissue-selective NIs and neurotoxicity (17,21). These tissue-specific protein cleavages, combined with other factors such as tissue-specific binding proteins with DRPLA or HD gene products, may further contribute to the tissue-specific distribution of NIs and neuronal degeneration (18). The present findings suggested that not only the tissue-specific cleavage activities or tissue-specific binding proteins with gene products, but also the promoter for the responsible gene itself is involved in determining the selective pattern of NI appearance and neuronal dysfunction.

The clinical symptoms of dragging of hind limbs, easily falling, truncal and limb ataxia in walking and impaired rotarod examinations can be attributed to the motor neuron dysfunction, cerebellar dysfunction and possibly the frontal lobe dysfunction, all of which were the regions developing the prominent polyQ NIs. However, the striking observation in our transgenic mice was the absence of neuronal cell death, apparent neuron loss, and reactive astrogliosis. These neuronal symptoms, therefore, derived from the dysfunction of neurons without neuronal cell death. Currently, it is considered that polyQ NIs are not linked to neuronal cell death (13,14,29). Apoptotic cell death has been demonstrated to be unrelated to the formation of NIs, particularly with those of ubiquitinated ones (13,14,29). However, it is not known how neuronal dysfunction without cell death is correlated to the NIs or to the process which induces NI formation. In our transgenic mouse model, appearance of NIs preceded the appearance of neuronal phenotype by 7 weeks, and neurological symptoms corresponded fairly well to the dysfunction of neurons where the NIs were prominently present. In other transgenic mice that do not show apparent neuronal cell death, the appearance of NIs similarly preceded the timing of neurological symptoms and correlated with dysfunction of neurons in the regions where the NIs were abundant (16,30). Further studies are needed to solve this issue, but polyQ itself has some neurotoxic effect leading to neuronal dysfunction in the neurons which eventually develop the NIs.

Table 1. Nuclear inclusions and transgene expression in the neural and non-neural tissues of transgenic mice (#543/#538)

Region	Inclusions (I)	Glial I	Neuronal I	Transgene expression[b]
Cerebrum				
Frontal cortex	+++	+++	+++	+++
Parietal cortex	+++	+++	++	++
Temporal cortex	++	++	++	+++
Occipital cortex	+/++	+/++	+/++	++
Basal ganglia	+/–	+/–	+/–	ND
Cerebellum	+++/++	+++	+++	++
Pons	+	+	+	ND
Ependyma	++			ND
Spinal cord	+++	+++/++	+/++	++
Pituitary	+++/–			+++/+
Kidney	–			–
Liver	–/+			–
Testis	–			–/+
Lung	++			++/+++
Muscle	–/+			–/+
Pancreas	–/++			ND
Heart	–			++
Eye	++			+++/++
Skin	+++			ND
Stomach	–			–
Intestine	–			–
Colon	–			–
Ovary	–			ND
Uterus	++[a]			++
Thymus	–			–
Spleen	–			–
Adrenal gland	–/+			ND
Peritoneum	++/+			++

For nuclear inclusions symbols are as follows: –, absent; +, detectable; ++, moderate; +++, abundant. When the abundancies for #543 and #538 differ, both grades are described, in the order #543/#538 (e.g. +++/++).

[a]Present in the peritoneal membrane.

[b]As for transgene expression assessed by RT–PCR, semi-quantitative grading of the expression level was scored from – to +++, according to the ratio of transgene RT–PCR products to β-actin RT–PCR products. –, absent; +, <0.2; ++, 0.2–0.5; +++, ≥0.5; ND, not determined. When the expression levels are different for #543 and #538, both grades are described, as for nuclear inclusions.

Interestingly, polyQ NIs occurred frequently in the glial cells in our mice. Glial NIs are rare in SBMA, but are occasionally found in the spinal cord of SBMA patients (M. Li and G. Sobue, unpublished data). In the DRPLA brain, glial NIs appear frequently (31). Glial NIs have not been well assessed in polyQ diseases, and thus glial cell involvement has not been considered to play a role in the pathogenesis of polyQ diseases. However, glial dysfunction may contribute to the development of neuronal dysfunction and degeneration, as observed in some neurodegenerative diseases or transgenic mouse models of SOD mutation with massive glial NIs (32,33), in which glutamate transporter expression in the astrocytes was decreased (33).

So far, several AR transgenic mouse models (34,35) with truncated or full-versions of the AR gene driven by neuron-specific promoters including the prion protein (PrP) and the neurofilament light chain (NF-L) promoters, and AR-YAC transgenic mice (36) have been reported. Neuronal phenotypes and NIs were documented only in those with potent promoters of PrP or NF-L-driven truncated AR containing a highly expanded CAG repeat (35). These observations suggested that high expression levels and relative dominance in polyQ content in the expressed AR protein with high expansion seem to be necessary to express the clinical and pathological phenotypes as demonstrated in the transgenic mouse models for other polyQ diseases (3,18,20).

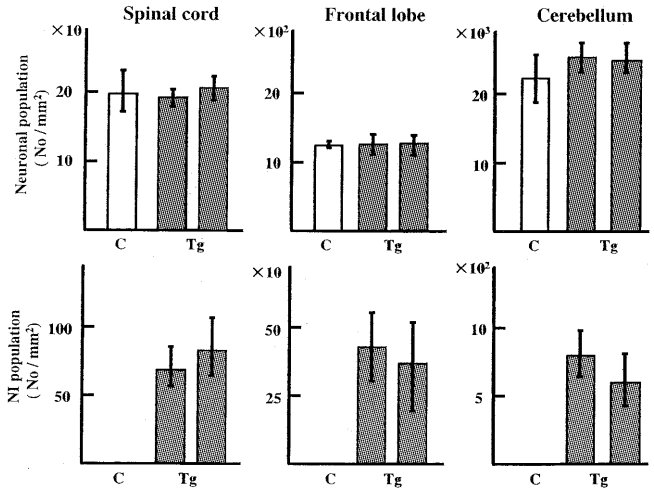

Figure 5. Population of NIs and neurons in the brain and spinal cord. Neuronal cell population in the lumbar spinal ventral horn, cerebral cortex of the frontal lobe and granular cell layers of the cerebellum in the transgenic mice was well preserved or even slightly elevated in the advanced stage at 12 weeks. The polyQ NIs were, however, abundantly present in these regions of transgenic mice. Results are expressed as mean ± SD for three mice. Open bars represent the littermate controls (C) and the shaded bars represent the transgenic (Tg) mice of #543 (left) and #538 (right). The differences in neuronal populations between the transgenic mice and their littermates are not statistically significant.

Taken together, in our transgenic mice the expression of an expanded pure polyQ without flanking sequences leads to neuronal dysfunction sufficient to induce a neurological phenotype. The disease process is caused by neuronal dysfunction rather than by primary neuronal cell death and subsequent neuron loss. In a recent *Drosophila* model that expressed expanded polyQ alone under the control of potent tissue-specific promoters (*elav*, *sev*, *gmr* and dpp^{blk}), severe retinal neurodegeneration and neuron loss were induced (37). This observation indicated that polyQ alone could cause neurotoxicity independent of its flanking sequences, which is in agreement with the present observations in our mouse model. However, in contrast to our model, the *Drosophila* model showed severe retinal neurodegeneration leading to neuron loss rather than neuronal dysfunction. This difference in polyQ neurotoxicity could be attributed to the promoters they used, but more probably to a difference in neuronal sensitivity; *Drosophila* retinal neurons could be more sensitive to polyQ-induced cytotoxicity.

What is the underlying molecular basis for the neuronal dysfunction without apparent neuronal cell death? The appearance of NIs in pancreatic islets caused cellular dysfunction without cell death, resulting in diabetes in HD transgenic mice (38,39), which suggested that cellular dysfunction similar to CNS can be present in peripheral organs. In addition, the transgenic mouse model for HD and SCA1 developed altered expression of neurotransmitter receptors (40) and several genes, including some enzymes and transcriptional factors (26), before apparent neurodegeneration. In the case of mutant AR with expanded polyQ, transcriptional alterations have been demonstrated in the *in vitro* system; the AR coactivator, ARA 24, differentially binds AR with different lengths of polyQ within AR resulting in weaker transactivation of AR (41). Reduced transcriptional regulatory competence, dependent on the length of polyQ in AR was also demonstrated in COS-1 cotransfection experiments (42,43). The CREB binding protein (44), which is sequestered in the AR aggregates in tissues of SBMA patients and neuronal cell lines expressing AR with expanded polyQ, develops altered transcriptional activity. These alterations, particularly of the trancriptional activity, may contribute to the impaired neuronal function before morphological neurodegeneration and neuronal cell death. In the transgenic mice that express exon 1 of the HD gene there are many neuropil aggregates located in the axon terminals and dendrites. These aggregates could also contribute to the early neuronal dysfunction that occurs before neuronal cell death (38,45,46). In our transgenic mice, neuropil aggregates were not observed, but brain weight was reduced and the neuronal population was well preserved. The morphological basis of neuronal dysfunction is not well understood, but neuronal atrophy, particularly of the retraction of the dendrites and axons, may be involved. Further morphometric study is needed to solve this issue.

The presence of a dysfunctional process without neuronal cell death is an important finding implying that SBMA and other polyQ-related disorders may be treated by amelioration of these dysfunctional processes. Our transgenic mice should help elucidate the molecular mechanism that underlies early phenotype expression from mutant AR. Further studies on transgenic mice expressing full-length AR cDNA with human AR promoter are now underway.

MATERIALS AND METHODS

Transgene construction

The 3.4 kb 5′-flanking region of the human AR gene was amplified by nested PCR from the human genomic DNA using the oligonucleotides 5′-CTGACTCTCAACCTGAC-3′ and 5′-GTCTTGGACGGCGGCCGAG-3′ first, and 5′-CTGAGAG-AACACCTCTGG-3′ and 5′-CCATCCTTGAGCTTGGCTG-3′ second. The 5′-flanking region of the human AR gene was subcloned in a pGEM-T vector (Promega). To prepare for an AR gene promoter-driven FLAG construct, we cut the CMV promoter out of the pFLAG-CMV-5c vector (Sigma). The 5′-flanking region of the human AR gene was liberated from the pGEM-T vector and subcloned into the treated pFLAG-CMV-5c vector (pFLAG/AR).

The 119 CAG repeat fragment was prepared from the pGEX-3X-119Q vector (kindly provided by Dr Fischbeck, NIH, MD) which includes the entire human AR gene with expanded 119 CAG repeats. From pGEX-3X-119Q clones, we liberated the 119 CAG repeat sequence using the restriction sites *Bsm*AI and *Pst*I which surround the CAG repeat. This resulted in the liberation of the complete 119 CAG repeat sequence with an additional G at the 5′-end and CA at the 3′-end, which potentially generates another CAG sequence at the junction when multiple copies are ligated in the same direction. The 119 CAG repeat fragment and the pFLAG/AR vector restricted by *ACC*65I and *Not*I were ligated and transformed. A single clone with an insert of ~720 bp was identified. Direct DNA sequencing confirmed that the 720 bp insert consisted of at least a 130 CAG repeat sequence from the 5′-end and also a

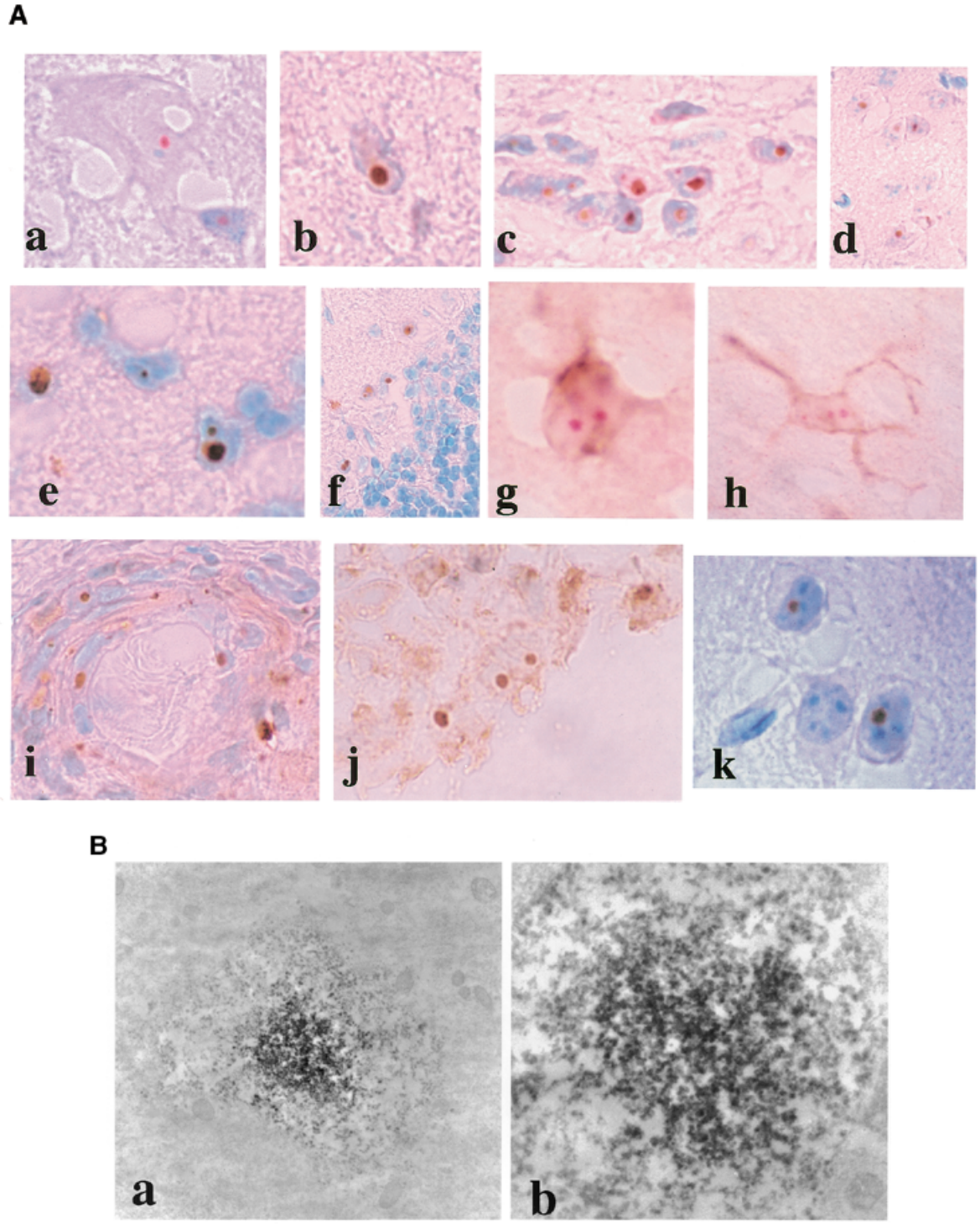

Figure 6. Light and electron microscopic immunohistochemical findings of NIs. (**A**) Immunohistochemistry of FLAG on NIs in the CNS of AR-239Q-#543 and #538 mice. FLAG NIs are observed in motor neurons of the lumbar spinal cord (a and b), cerebral cortex of the frontal lobe (c and d) and cerebellar molecular and granular cell layers (e and f). NIs are observed in the motor neurons (a) and glial cells (b) in the spinal cord, and are also found in the neurons as well as glial cells in the frontal cortex and cerebellum (c–f). In the cerebellum, NIs are not found in the Purkinje cell nuclei and are restricted to the neurons and glial cells in the molecular and granular cell layers. NIs in the astrocyte nuclei were confirmed by double staining for FLAG (red) and GFAP (brown) in the lumbar spinal cord (g) and cerebral cortex of the frontal lobe (h). NIs are also present in the visceral organs such as the epidermal cells of the skin (i) and the epithelial cells of the lung (j). The nuclear inclusions are heavily ubiquitinated (k). Magnification, 600~1000×. (**B**) Electron microscopic immunohistochemical features of the NIs in the astrocyte in the cerebral cortex of 12-week-old AR-239Q-#543 mice. Dense granular aggregates of FLAG-immunoreactive material without a limiting membrane or fibrous configurations are found (a and b) Magnification: a, 10 000×; b, 20 000×.

130 CTG sequence from the 3′-end which proves the insertion of a 239 CAG repeat sequence (119 CAG × 2 copies plus 1 CAG at the junction).

Generation and maintenance of transgenic mice and genotyping

Transgenic mice were generated by microinjection of single cell SJL×C57BL/6 embryos. Of 90 newborn mice, four founder transgenic lines were obtained; two males and two females. These founders were initially backcrossed to C57BL/6J. Mouse tail DNA was screened by PCR for the presence of the transgene using the primers 5′-GGCAGTCAGGTCTTCAG-TAGC-3′ and 5′-GATGCGGTAGTCGCTGCAGC-3′, and the confirmation of the CAG repeat size using the primers 5′-GCCTGTTGAACTCTTCTGAGC-3′ and 5′-GGTCACA-GGGATGCCACC-3′. The transgene copy number in each line was determined by densitometric comparison of Southern blot hybridization intensity of FLAG DNAs with known standards using enzymes cutting only once in the transgene. Mice were housed in a conventional facility. For determining the CAG repeat size, the PCR products (~830 bp in size) were amplified with a Texas Red-labeled primer and electrophoresed on a 6% denaturing polyacrylamide gel for 12 h using an autosequencer (5500 DNA sequencer, Hitachi).

Assessment of motor ability

Motor ability was assessed on a weekly basis using a rotarod apparatus. The period for which a mouse could remain on a rotating axle (3.6 cm diameter; speed of rotation, 16 r.p.m.) without falling was measured as described previously (47). The test was stopped after an arbitrary limit of 180 s and was the requirement for three sessions of training, or habituation, before non-transgenic mice attained stable performance.

RNA and protein expression analyses

Animals were anesthetized with diethyl ether and exsanguinated. Tissues were carefully and quickly removed and snap-frozen in liquid nitrogen. Total RNA was extracted from tissues with Trizol (Life Technologies/Gibco BRL), and was reverse transcribed using SUPERSCRIPT II reverse transcriptase (Life Technologies/Gibco BRL) according to the standard protocol. Primers for specific transgene RNA detection were 5′-CGACGATGACAAGTAGCTCG-3′ and 5′-GGACAAGGCTGGTGGGCAC-3′. After amplification, the products were separated by agarose gel electrophoresis. The intensity of the signals of the PCR products stained with ethidium bromide was quantified using a CCD image analyzer (Gel Doc 1000, Bio-Rad) and normalized against β-actin mRNA levels. To ascertain that products were derived from mRNAs with no contamination from genomic sequences, we performed PCR using RNA which had not been reverse transcribed.

Frozen tissue (0.1 g wet weight) was homogenized in 1000 µl of 50 mM Tris pH 8.0, 150 mM NaCl, 1% NP-40, 0.5% deoxycholate, 0.1% SDS and 1 mM 2-mercaptoethanol with 1 mM PMSF and aprotinin at 6 µg/ml. Homogenates were sonicated on ice for 15 s and spun at 2500 *g* for 30 min at 4°C. The pellet and supernatant fractions were obtained. Each lane on a 5–20% SDS–PAGE gel was loaded with 20 µl of protein from each fraction. Kaleidoscope prestained standards were used as size markers (Bio-Rad). Proteins were transferred to Hybond-P membranes (Amersham). After immunoprobing with the antibody, rabbit anti-octapeptide epitope tag (Zymed) at a 1:2000 dilution, second antibody probing and detection were performed using the ECL kit (Amersham).

Light and electron microscopic immunohistochemistry

Animals were anesthetized with diethyl ether and exsanguinated. They were perfused through the left cardiac ventricle with 40 ml of a 4% paraformaldehyde fixative in phosphate buffer (pH 7.4). Tissues were carefully removed and placed into fixative for 4 h before being transferred to 10, 15 and 20% sucrose, consecutively, in 0.01 M PBS (pH 7.4) for 4 h each at 4°C. Tissues were mounted in Tissue-Tek OCT compound (Sakura) and frozen with powdered CO_2 in acetone. Cryostat sections, 6 µm thick, were prepared from the frozen tissues, blocked with normal animal serum (1:20) and incubated with antibodies: goat anti-OctA-probe(D-8)-G (1:200) (Santa Cruz Biotechnology), rabbit anti-GFAP (ready-to-use) (Dako), rabbit anti-ubiquitin (1:400; Dako), and rabbit anti-proteasomes: 20s, PA28α and PA28γ (1:2000) (Affiniti Research Products). Samples were then incubated with biotinylated anti-species-specific IgG (Vectastain, Elite ABC Kit). Endogenous peroxidase was blocked by preincubation of tissue sections with 0.3% H_2O_2 in methanol for 30 min. Immune complexes were visualized using streptavidin-horseradish peroxidase (Dako) and 3,3′-diaminobenzidine (Dojindo) substrate. Sections were counterstained with methyl green.

For paraffin-embedded samples, animals were anesthetized and perfused as described above, and the tissues processed. Then 4 µm tissue sections were deparaffinized, dehydrated with alcohol and heated at 121°C for 15 min. The tissue sections were processed in the same way as the frozen sections.

Double-labeling immunohistochemistry was performed with two primary antibodies: rabbit anti-GFAP (Dako) and goat anti-OctA-probe (D-8)-G (1:200) (Santa Cruz). Sections were preincubated with 3% H_2O_2 in methanol, and then with normal horse serum diluted in 0.05 M Tris buffer (pH 7.6) containing bovine serum albumin. The sections were then incubated with goat anti-OctA-probe (D-8)-G (1:400) (Santa Cruz) at 4°C overnight, washed with 0.05 M TBS buffer, and incubated with biotinylated horse anti-goat IgG, stained with streptavidin-alkaline phosphatase, and visualized with fast-red. The rabbit polyclonal antibody against GFAP was subsequently applied to sections for 2 h at room temperature. After washing, the sections were incubated with horseradish peroxidase-labeled donkey anti-rabbit Ig $F(ab')_2$ which had demonstrated no cross-reaction with either goat or horse sera (Amersham), and visualized with 3,3′-diaminobenzidine.

For electron microscopic immunohistochemistry, buffered formalin-fixed, paraffin-embedded tissue sections were immunostained with anti-OctA-probe(D-8)-G (1:100) (Santa Cruz), then incubated and visualized by the same method as the frozen sections. They were fixed with 2% osmium tetroxide in 0.1% cacodylic acid sodium buffer (pH 7.4), dehydrated in an alcohol gradient and embedded in epoxy resin, from which ultrathin sections were obtained. They were observed under an electron microscope (Hitachi H-7000, Hitachi).

Terminal deoxynucleotidyltransferase-mediated UTP end-labeling (TUNEL)

Cryostat sections were used for terminal deoxynucleotidyltransferase catalyzed incorporation of digoxigenin-dUTP into the free 3′-OH terminii of fragmented DNA (Intergen). The incorporated digoxigenin-dUTP was detected with a peroxidase-conjugated anti-digoxigenin antibody. Sites of enzymatic activity were visualized with H_2O_2 and 3,3′-diaminobenzidine. Sections from normal female mouse mammary gland 3 days after weaning of pups were used as positive controls; negative controls were sections from 12-week-old non-transgenic littermates.

Quantification of NIs and neuronal population in the brain and spinal cord

For assessment of neuronal populations and the NIs, 4 μm thick coronal sections of the frontal cortex and cerebellum stained by the Nissle method and anti-OctA-probe(D-8)-G (1:200) (Santa Cruz) were prepared, and the number of NIs and neurons with obvious nucleolus within a 0.292 mm^2 area for each individual mouse was counted using a light microscope with a computer-assisted image analyzer (Luzex FS Nikon). For assessment of the neuronal populations in the ventral horn of the spinal cord, 10 transverse sections of the 4th lumbar spinal cord were prepared and all neurons larger than 30 μm in diameter with an obvious nucleolus, present within the ventral horn, were counted as described previously (48). The immunoreactive NIs in the spinal ventral horns were similarly assessed. Populations of NIs and neurons were expressed as the number per square millimeter.

ACKNOWLEDGEMENTS

We thank Thomas Saunders and the Michigan Transgenic Animal Model Core for helping to make the transgenic mice. We are grateful to Drs K. Sawada, T. Yoshihara and N. Hishikawa for their excellent support in the experimental procedure. This work was supported by a COE grant from the Ministry of Education, Culture, Sports, Science and Technology of Japan, and grants from the Ministry of Health, Labour and Welfare of Japan.

REFERENCES

1. La Spada, A.R., Wilson, E.M., Lubahn, D.B., Harding, A.E. and Fischbeck, K.H. (1991) Androgen receptor gene mutations in X-linked spinal and bulbar muscular atrophy. *Nature*, **352**, 77–79.
2. Perutz, M.F. (1999) Glutamine repeats and neurodegenerative diseases: molecular aspects. *Trends Biochem. Sci.*, **24**, 58–63.
3. Reddy, H.P., Williams, M. and Tagle, D.A. (1999) Recent advances in understanding the pathogenesis of Huntington's disease. *Trends Neurosci.*, **22**, 248–255.
4. Kennedy, W.R., Alter, M. and Sung, J.H. (1968) Progressive proximal spinal and bulbar muscular atrophy of late onset: a sex-linked recessive trait. *Neurology*, **18**, 671–680.
5. Sobue, G., Hashizume, Y., Mukai, E., Hirayama, M. and Takahashi, A. (1989) X-linked recessive bulbospinal neuronopathy, a clinicopathological study. *Brain*, **112**, 209–232.
6. Doyu, M., Sobue, G., Mukai, E., Kachi, T., Yasuda, T., Mitsuma, T. and Takahashi, A. (1992) Severity of X-linked recessive bulbospinal neuronopathy correlates with the size of the tandem CAG repeat in androgen receptor gene. *Ann. Neurol.*, **32**, 707–710.
7. Igarashi, S., Tanno, Y., Onodera, O., Yamazaki, M., Sato, S., Ishikawa, A., Miyatani, N., Nagashima, M., Ishikawa, Y., Sahashi, K. *et al.* (1992) Strong correlation between the number of CAG repeats in androgen receptor genes and clinical onset of spinal and bulbar muscular atrophy. *Neurology*, **42**, 2300–2302.
8. La Spada, A.R., Roling, D.B., Harding, A.E., Warner, C.L., Spiegel, R., Hausmanowa-Petrusewicz, I., Yee, W.C. and Fischbeck, K.H. (1992) Meiotic stability and genotype–phenotype correlation of the trinucleotide repeat in X-linked spinal and bulbar muscular atrophy. *Nat. Genet.*, **2**, 301–304.
9. Li, M., Miwa, S., Kobayashi, Y., Merry, D.E., Yamamoto, M., Tanaka, F., Doyu, M., Hashizume, Y., Fischbeck, K.H. and Sobue, G. (1998) Nuclear inclusions of the androgen receptor protein in spinal and bulbar muscular atrophy. *Ann. Neurol.*, **44**, 249–254.
10. Li, M., Nakagomi, Y., Kobayashi, Y., Merry, D.E., Tanaka, F., Doyu, M., Mitsuma, T., Hashizume, Y., Fischbeck, K.H. and Sobue, G. (1998) Non-neural nuclear inclusions of androgen receptor protein in spinal and bulbar muscular atrophy. *Am. J. Pathol.*, **153**, 695–701.
11. Kobayashi, Y., Kume, A., Li, M., Doyu, M., Hata, M., Ohtsuka, K. and Sobue, G. (2000) Chaperones Hsp70 and Hsp40 suppress aggregate formation and apoptosis in cultured neuronal cells expressing truncated androgen receptor protein with expanded polyglutamine tract. *J. Biol. Chem.*, **275**, 8772–8778.
12. Stenoien, D.L., Cummings, C.J., Adams, H.P., Mancini, M.G., Patel, K., DeMartino, G.N., Marcell, M., Weigel, N.L. and Mancini, M.A. (1999) Polyglutamine-expanded androgen receptors form aggregates that sequester heat shock proteins, proteasome components and SRC-1, and are suppressed by the HDJ-2 chaperone. *Hum. Mol. Genet.*, **8**, 731–741.
13. Saudou, F., Finkbeiner, S., Devys, D. and Greenberg, M.E. (1998) Huntingtin acts in the nucleus to induce apoptosis but death does not correlate with the formation of intranuclear inclusions. *Cell*, **95**, 55–66.
14. Simeoni, S., Mancini, M.A., Stenoien, D.L., Marcelli, M., Weigel, N.L., Zanisi, M., Martini, L. and Poletti, A. (2000) Motoneuronal cell death is not correlated with aggregate formation of androgen receptors containing an elongated polyglutamine tract. *Hum. Mol. Genet.*, **9**, 133–144.
15. Faber, P.W., Alter, J.R., MacDonald, M.E. and Hart, A.C. (1999) Polyglutamine-mediated dysfunction and apoptotic death of a *Caenorhabditis elegans* sensory neuron. *Proc. Natl Acad. Sci. USA*, **96**, 179–184.
16. Mangiarini, L., Sathasivam, K., Seller, M., Cozens, B., Harper, A., Hetherington, C., Lawton, M., Trottier, Y., Lehrach, H., Davies, S.W. *et al.* (1996) Exon 1 of the *HD* gene with an expanded CAG repeat is sufficient to cause a progressive neurological phenotype in transgenic mice. *Cell*, **87**, 493–506.
17. Hodgson, J.G., Agopyan, N., Gutekunst, C.-A., Leavitt, B.R., LePiane, F., Singaraja, R., Smith, D.J., Bissada, N., McCutcheon, K., Nasir, J. *et al.* (1999) A YAC mouse model for Huntington's disease with full-length mutant huntingtin, cytoplasmic toxicity, and selective striatal neurodegeneration. *Neuron*, **23**, 181–192.
18. Reddy, P.H., Williams, M., Charles, V., Garrett, L., Pike-Buchanan, L., Whestell, W.O., Miller, G. and Tagle, D.A. (1998) Behavioural abnormalities and selective neuronal loss in HD transgenic mice expressing mutated full-length *HD* cDNA. *Nat. Genet.*, **20**, 198–202.
19. Burright, E.N., Clark, H.B., Servadio, A., Matilla, T., Feddersen, R.M., Yunis, W.S., Duvick, L.A., Zoghbi, H.Y. and Orr, H.T. (1995) SCA1 transgenic mice: a model for neurodegeneration caused by an expanded CAG trinucleotide repeat. *Cell*, **82**, 937–948.
20. Ikeda, H., Yamaguchi, M., Sugai, S., Aze, Y., Narumiya, S., and Kakizuka, A. (1996) Expanded polyglutamine in the Machado–Joseph disease protein induces cell death *in vitro* and *in vivo*. *Nat. Genet.*, **13**, 196–202.
21. Schilling, G., Wood, J.D., Duan, K., Slunt, H.H., Gonzales, V., Yamada, M., Cooper, J.K., Margolis, R.L., Jenkins, N.A., Copeland, N.G. *et al.* (1999) Nuclear accumulation of truncated atrophin-1 fragments in a transgenic mouse model of DRPLA. *Neuron*, **24**, 275–286.
22. Shelbourne, P.F., Killeen, N., Hevner, R.F., Johnston, H.M., Tecott, L., Lewandoski, M., Ennis, M., Ramirez, L., Li, Z., Lannicola, C. *et al.* (1999) A Huntington's disease CAG expansion at the murine *Hdh* locus is unstable and associated with behavioural abnormalities in mice. *Hum. Mol. Genet.*, **8**, 763–774.
23. Yvert, G., Lindenberg, K.S., Picaud, S., Landwehrmeyer, G.B., Sahel, J.-A. and Mandel, J.-L. (2000) Expanded polyglutamines induce neurodegeneration and trans-neuronal alterations in cerebellum and retina of SCA7 transgenic mice. *Hum. Mol. Genet.*, **9**, 2491–2506.

24. Tumaine, M., Razza, A., Mahal, A., Mangiarini, L., Bates, G. and Davies, S.W. (2000) Nonapoptotic neurodegeneration in a transgenic mouse model of Huntington's disease. *Proc. Natl Acad. Sci. USA*, **97**, 8093–8097.
25. Bates, G.P., Mangiarini, L. and Davies, S. (1998) Transgenic mice in the study of polyglutamine repeat expansion diseases. *Brain Pathol.*, **8**, 699–714.
26. Lin, X., Antalffy, B., Kang, D., Orr, H.T. and Zoghbi, H.Y. (2000) Polyglutamine expansion down-regulates specific neuronal genes before pathologic changes in SCA1. *Nat. Neurosci.*, **3**, 157–163.
27. Takeda, H., Chodak, G., Mutchnik, S., Nakamoto, T. and Chang, C. (1989) Immunohistochemical localization of androgen receptors with mono- and polyclonal antibodies to androgen receptor. *J. Endocrinol.*, **126**, 17–25.
28. Tanaka, F., Reeves, M., Ito, Y., Matsumoto, M., Li, M., Miwa, S., Inukai, A., Yamamoto, M., Doyu, M., Yoshida, M. *et al*. (1999) Tissue-specific somatic mosaicism in spinal and bulbar muscular atrophy is dependent on CAG-repeat length and androgen receptor-gene expression level. *Am. J. Hum. Genet.*, **65**, 966–973.
29. Klement, I.A., Skinner, P.J., Kaytor, M.D., Yi, H., Hersch, S.M., Clark, H.B., Zoghbi, H.Y. and Orr, H.T. (1998) Ataxin-1 nuclear localization and aggregation: role in polyglutamine-induced disease in *SCA1* transgenic mice. *Cell*, **95**, 41–53.
30. Davies, S.W., Turmaine, M., Cozens, B.A., DiFiglia, M., Sharp, A.H., Ross, C.A., Scherzinger, E., Wanker, E.E., Mangiarini, L. and Bates, G.P. (1997) Formation of neuronal intranuclear inclusions underlies the neuronal dysfunction in mice transgenic for the HD mutation. *Cell*, **90**, 537–548.
31. Hayashi, Y., Kakita, A., Yamada, M., Koide, R., Igarashi, S., Takano, H., Ikeuchi, T., Wakabayashi, K., Egawa, S., Tsuji, S. *et al*. (1998) Hereditary dentatorubral-pallidoluysian atrophy: detection of widespread ubiquitinated neuronal and glial intranuclear inclusions in the brain. *Acta Neuropathol. (Berl.)*, **96**, 547–552.
32. Bruijn, L.I., Becher, M.W., Lee, M.K., Anderson, K.L., Jenkins, N.A., Copeland, N.G., Sisodia, S.S., Rothstein, J.D., Borchelt, D.R., Price, D.L. *et al*. (1997) ALS-linked SOD1 mutant G85R mediates damage to astrocytes and promotes rapidly progressive disease with SOD1-containing inclusions. *Neuron*, **18**, 327–338.
33. Jellinger, K.A. (1998) Dementia with grains (argyrophilic grain disease). *Brain Pathol.*, **8**, 377–386.
34. Bingham, P.M., Scott, M.O., Wang, S., McPhaul, M.J., Wilson, E.M., Garbern, J.Y., Merry, D.E. and Fischbeck, K.H. (1995) Stability of an expanded trinucleotide repeat in the androgen receptor gene in transgenic mice. *Nat. Genet.*, **9**, 191–196.
35. Merry, D.E., Woods, J., Walcott, J., Bish, L., Fischbeck, K.H. and Abel, A. (1999) Characterization of a transgenic model for SBMA. *Am. J. Hum. Genet.*, **65** (Suppl.), A30.
36. La Spada, A.R., Peterson, K.R., Meadows, S.A., McClain, M.E., Jeng, G., Chmelar, R.S., Haugen, H.A., Chen, K., Singer, M.J., Moore, D. *et al*. (1998) Androgen receptor YAC transgenic mice carrying CAG 45 alleles show trinucleotide repeat instability. *Hum. Mol. Genet.*, **7**, 959–967.
37. Marsh, J.L., Walker, H., Theisen, H., Zhu, Y.-Z., Fielder, T., Purcell, J. and Thompson, L.M. (2000) Expanded polyglutamine peptide alone are intrinsically cytotoxic and cause neurodegeneration in *Drosophila*. *Hum. Mol. Genet.*, **9**, 13–25.
38. Sathasivam, K., Hobbs, C., Turmaine, M., Mangiarini, L., Mahal, A., Bertaux, F., Wanker, E.E., Dohert, P., Davies, S.W. and Bates, G.P. (1999) Formation of polyglutamine inclusions in non-CNS tissue. *Hum. Mol. Genet.*, **8**, 813–822.
39. Hurlbert, M.S., Zhou, W., Wasmeier, C., Kaddis, F.G., Hutton, J.C. and Freed, C.R. (1999) Mice transgenic for an expanded CAG repeat in the Huntington's disease gene develop diabetes. *Diabetes*, **48**, 649–651.
40. Cha, J.J., Kosinski, C.M., Kerner, J.A., Alsdorf, S.A., Mangiarini, L., Davies, S.W., Penney, J.B., Bates, G.P. and Young, A.B. (1998) Altered brain neurotransmitter receptors in transgenic mice expressing a protein of an abnormal human Huntington disease gene. *Proc. Natl Acad. Sci. USA*, **95**, 6480–6485.
41. Hsiao, P.-W., Lin, D.-L., Nakao, R. and Chang, C. (1999) The linkage of Kennedy's neuron disease to ARA24, the first identified androgen receptor polyglutamine region-associated coactivator. *J. Biol. Chem.*, **274**, 20229–20234.
42. Mhatre, A.N., Trifiro, M.A., Kaufman, M., Kazemi-Esfarjani, P., Figlewicz, D., Rouleau, G. and Pinsky, L. (1993) Reduced transcriptional regulatory competence of the androgen receptor in X-linked spinal and bulbar muscular atrophy. *Nat. Genet.*, **5**, 184–188.
43. Kazemi-Esfarjani, P., Trifiri, M.A. and Pinsky, L. (1995) Evidence for a repressive function of the long polyglutamine tract in the human androgen receptor: possible pathogenetic relevance for the (CAG)n-expanded neuronopathies. *Hum. Mol. Genet.*, **4**, 523–527.
44. McCampbell, A., Taylor, J.P., Taye, A.A., Robitschek, J., Li, M., Walcott, J., Merry, D., Chai, Y., Paulson, H., Sobue, G. and Fischbeck, K.H. (2000) CREB-binding protein sequestration by expanded polyglutamine. *Hum. Mol. Genet.*, **9**, 2197–2202.
45. Li, H., Li, S.-H., Cheng, A.L., Mangiarini, L., Bates, G.P. and Li, X.-J. (1999) Ultrastructural localization and progressive formation of neuropil aggregates in Huntington's disease transgenic mice. *Hum. Mol. Genet.*, **8**, 1227–1236.
46. Gutekunst, C.-A., Li, S.-H., Yi, H., Mulroy, J.S., Kuemmerle, S., Jones, R., Rye, D., Ferrante, R.J., Hersch, S.M. and Li, X.-J. (1999) Nuclear and neuropil aggregates in Huntington's disease: relation to neuropathology. *J. Neurosci.*, **19**, 2522–2534.
47. Barneoud, P., Lolivier, J., Sanger, D.J., Scatton, B. and Moser, P. (1997) Quantitative motor assessment in FALS mice: a longitudinal study. *Neuroreport*, **8**, 2861–2865.
48. Terao, S., Sobue, G., Li, M., Hashizume, Y., Tanaka, F. and Mitsuma, T. (1996) The lateral corticospinal tract and spinal ventral horn in X-linked recessive spinal and bulbar muscular atrophy: a quantitative study. *Acta Neuropathol. (Berl.)*, **93**, 1–6.